Research Article

Near-Infrared All-Silicon Photodetectors

M. Casalino, G. Coppola, M. Iodice, I. Rendina, and L. Sirleto

Institute for Microelectronics and Microsystems, National Council of Research, Via P. Castellino 111, 80131 Naples, Italy

Correspondence should be addressed to M. Casalino, maurizio.casalino@na.imm.cnr.it

We report the fabrication and characterization of all-silicon photodetectors at 1550 nm based on the internal photoemission effect. We investigated two types of structures: bulk and integrated devices. The former are constituted by a Fabry-Perot microcavity incorporating a Schottky diode, and their performance in terms of responsivity, free spectral range, and finesse was experimentally calculated in order to prove an enhancement in responsivity due to the cavity effect. Results show a responsivity peak of about 0.01 mA/W at 1550 nm with a reverse bias of 100 mV. The latter are constituted by a Schottky junction placed transversally to the optical field confined into the waveguide. Preliminary results show a responsivity of about 0.1 mA/W at 1550 nm with a reverse bias of 1 V and an efficient behaviour in both C and L bands. Finally, an estimation of bandwidth for GHz range is deduced for both devices. The technological steps utilized to fabricate the devices allow an efficiently monolithic integration with complementary metal-oxide semiconductor (CMOS) compatible structures.

1. Introduction

Silicon is an extremely attractive platform for large-scale integration of multiple optical and electronic functions on a single silicon chip. This should result in revolutionizing applications in microelectronics, telecommunications, and biological and chemical sensing. Significant advantages exist when using silicon as the base material for such devices: in particular, a vast amount of research is now available to designers and process engineers on all aspects of the material system, as well as the established, global silicon processing industry that has evolved from almost six decades of silicon-based microelectronics fabrication. Silicon wafers have the lowest cost per unit area and the highest crystal quality of any semiconductor material. The industry is able to produce microprocessors with hundreds of millions of components— all integrated onto thumb-sized chips—and offers them at such low prices that they are increasingly used in consumer electronics. Silicon manufacturing represents the most spectacular convergence of technological sophistication and economics of scale [1–3].

For these reasons, in the last two decades, there has been growing interest in photonic devices based on Si-compatible materials [4] in the field of both the optical telecommunications and the optical interconnection. In this contest, tremendous progress in the technological processes based on the use of silicon-on-insulator (SOI) substrates has allowed to obtain reliable and fully effective CMOS-compatible optical components such as: low loss waveguides, high-Q resonators, high-speed modulators, couplers, and optically pumped lasers [5–10]. All these devices have been developed to operate in the wavelength range from C band (1528–1561 nm) to L band (1561–1620 nm) where the defect-free intrinsic bulk silicon has minimal absorption. On the other hand, this transparency window limits silicon applications for photodetection in the infrared range so that the development of high-performance waveguide-integrated photodetectors on Si-CMOS platform has remained an imperative but unaccomplished task so far.

In order to detect light into C and L bands, germanium-based photodetectors have shown impressive advances during the last years. However, the aggressive substrate cleaning processes and thermal mismatch between Ge and Si hinder a seamless integration of Ge-PDs with the standard Si-integrated circuit realization. For these reasons their fabrication and related technologies are much more expensive than silicon-based PDs [11, 12].

In order to develop all-silicon photodetectors and to take advantage of low-cost standard Si-CMOS processing technologies without additional material or process steps, a number of options have been proposed [13], in particular, the two-photon absorption [14], the incorporation of optical dopants/defects with midbandgap energy levels into the Si lattice [15, 16], the internal photoemission effect (IPE) [17], recently adopted also in silicon photodetectors based on surface plasmons [18, 19].

The aim of this work is to investigate photodetectors based on IPE at near-infrared wavelengths. We report the fabrication and characterization of two types of structures: bulk and integrated devices. The performance in terms of responsivity and estimated bandwidth is reported and discussed.

2. Internal Photoemission Theory

Internal photoemission is the optical excitation of electrons into the metal to an energy above the Schottky barrier and then transport of these electrons to the conduction band of the semiconductor (Figure 1).

The standard theory of photoemission from a metal into a vacuum is due to Fowler [20]. Fowler's theory was originally obtained without taking into account the thickness of the Schottky metal layer. In order to study the quantum efficiency for thin metal films, the theory must be further extended, taking into account multiple reflections of the excited electrons from the surfaces of the metal film, in addition to collisions with phonons, imperfections, and cold electrons. Assuming a thin metal film, a phenomenological semiclassical ballistic transport model for the effects of the scattering mechanisms resulting in a multiplicative factor for quantum efficiency has been developed by Vickers [21].

The efficiency in collecting those electrons which have sufficient normal kinetic energy to overcome potential barrier (Φ_B) will depend on their probability of collisions with cold or hot electrons and with the two boundary surfaces of the metal. Supposing that the Schottky barrier is illuminated through the front surface of the metal electrode and that optical absorption is uniform throughout the metal thickness, we indicate with p_t the average probability that photoexcited electrons arrive at the semiconductor surface without collision. Then, we indicate with p_r the accumulated probability of arrival at the reflection boundary of those electrons which have sufficient energy to overcome Φ_B after one collision with cold or hot electrons, which are oriented with equal probability over the entire half-sphere before reflection by the metal surface. Finally, for multiple reflections, we indicate with p the probability that the capturable electrons can bounce from one metal boundary to another. Therefore, the total accumulated probability that the electrons will have sufficient normal kinetic energy to overcome Φ_B is given by [22]

$$P_E = p_t + p_r \left(1 + p + p^2 + p^3 + \cdots\right) \exp\left(-\frac{d}{L}\right)$$
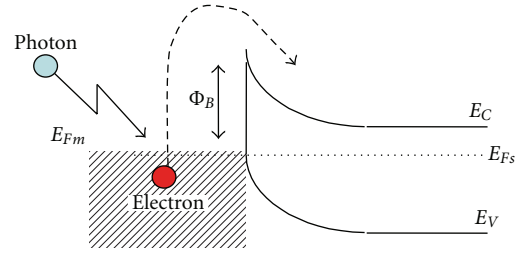$$\cong \frac{L}{d}\left[1 - e^{-d/L}\right]^{1/2}, \tag{1}$$

Figure 1: Energy band diagram for a metal-semiconductor junction.

where d is the metal thickness and L the mean free path describing the probability of collision with cold or hot electrons [22]. It would be possible to show by plotting (1) that by decreasing metal thickness d P_E increases and that a considerable gain can be obtained when d is much smaller than L (thin film). This gain is due to the increased probability of emission of carriers. In a recent work, Scales and Berini show that a further enhancement of this probability emission can be obtained in structures realized with thin metal film buried in a semiconductor and forming two Schottky barriers [23].

3. IPE-Based Bulk Device

3.1. Proposed Device. The sketch of the proposed device is shown in Figure 2. The resonant cavity is a vertical-to-the-surface Fabry-Perot structure. It is formed by a buried reflector, a top mirror interface and, in the middle, a silicon cavity. The buried reflector is a Bragg mirror, realized by alternating layers of amorphous hydrogenated silicon (a-Si:H) and silicon nitride (Si_3N_4). A thick copper (Cu) Schottky metal layer, working as both top reflector and absorbing medium, is deposited above the silicon substrate. Schottky Cu is surrounded by an aluminum (Al) contact in order to collect the photogenerated carriers.

Due to the multiple reflections of the optical field inside the cavity an improvement in metal absorbance, thus in responsivity, is expected.

3.2. Device Fabrication. The samples were fabricated starting from a slightly doped (10^{12} cm^{-3}) p-type bi-polished $100\,\mu$m thick silicon wafer. On the back, a multilayer Bragg mirror is fabricated by plasma-enhanced chemical vapor deposition technique (PECVD). The mirror is composed by a quarter-wave stack of a-Si:H and Si_3N_4 layers, having nominal refractive index, at 1550 nm, of 3.52 and 1.82, respectively. The reflector is realized with five periods of a-Si:H/Si_3N_4 pairs, whose nominal thickness is 110 nm and 213 nm, respectively. Silicon nitride is deposited at pressure of 1.2 mbar, temperature of 250°C, at 30 W of RF power. In the deposition chamber 10 sccm of NH_3, 88 sccm of SiH_4 (5% in He), and 632 sccm of N_2 are flowed. The deposition rate is 22.93 nm/min, and the suited Si_3N_4 thickness is obtained with a process time of 9 min and 17 sec. Amorphous hydrogenated silicon, instead, is deposited at pressure of 0.8 mbar, temperature of 250°C, power of 2 W, and a SiH_4
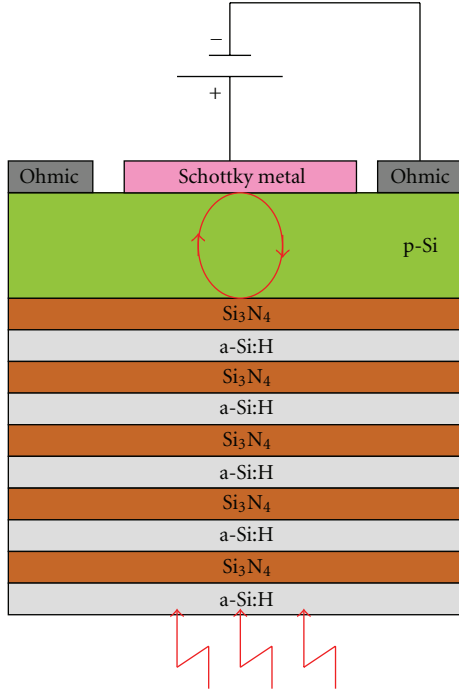
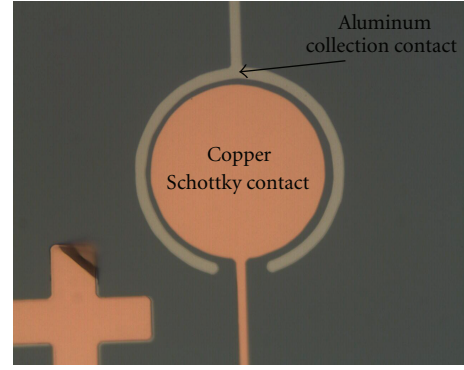FIGURE 2: Schematic cross-section of the proposed photodetector.
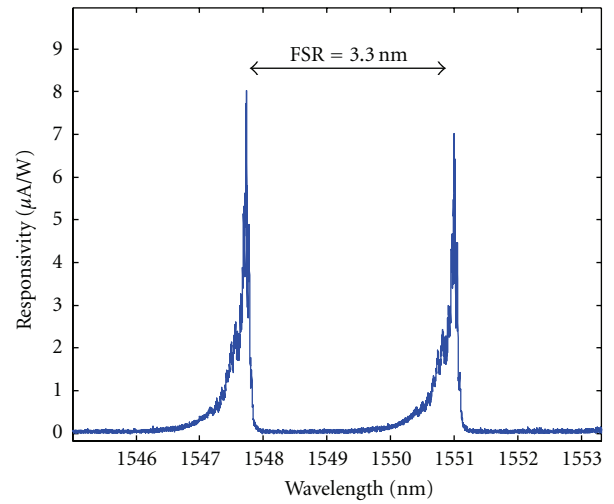

FIGURE 3: Top view of the proposed fabricated device.

FIGURE 4: Measured external responsivity versus wavelength for the proposed Cu/p-Si photodetector at −100 mV.

(5% in He) flow of 600 sccm. The a-Si:H deposition rate is 3.15 nm/min, and the desired thickness is obtained with a process time of 34 min and 56 sec. The collecting ohmic contact and the Schottky contact were both realized on the top of the sample. The collecting contact was made by a 200 nm thick aluminum film, thermally evaporated at $3 \cdot 10^{-6}$ mbar and 150°C, patterned by a lift-off process of photoresist Shipley S1813 which, deposited by a spin coater at 4000 rpm, has a thickness of 1.4 μm. Then, an annealing at 475°C in nitrogen for 30 min, in order to get a nonrectifying behavior, was carried out [24]. Finally, the Schottky contact was fabricated. Copper was thermally evaporated and patterned by lift-off, so obtaining a metal film thickness of 200 nm, thicker than field penetration depth. The collecting contact and the Schottky contact are shaped by a ring and a disk (40 μm of radius) with the Schottky metal disk placed inside the ohmic metal ring (Figure 3).

3.3. Responsivity Measurements. The experimental setup for external responsivity measurements is quite simple. The laser beam emitted by a wavelength tunable laser is split by a Y fiber junction. One branch is used to monitor the optical power, while the other one is collimated, chopped, and sent onto the device. The photocurrent produced by our device is measured by a lock-in amplifier. A transimpedance amplifier (TIA) is employed to provide a reverse bias voltage to the photodetector and at the same time for reducing the dark current. The dark current cancellation circuit realised by using a transimpedance amplifier has a limited bandwidth; however it is adequate for our scope, that is dc or quasistatic measurements [25].

Measurements around 1550 nm (step of 0.001 nm) at 100 mV of reverse bias applied were carried out (Figure 4). At 100 mV of the reverse bias applied, device dark current is about 0.4 μA.

We observed two distinct peaks indicating the influence of the cavity. The measured free spectral range of 3.3 nm agrees with the value calculated by the formula FSR = $\lambda_0^2/(2nL)$ [26], where λ_0 is the central wavelength at the considered range (1550 nm), n is the silicon cavity refractive index (3.48 at 1550 nm [27]), and L is the silicon cavity thickness (100 μm). A peak external responsivity and an experimental finesse of 8.2 μA/W and 33, respectively, are obtained.

In our previous paper [28], a macroscopic device (radius of about 2 mm) was considered and peak external responsivity value of 4.3 μA/W and a finesse value of 4.7 were reported. In this paper, a microscopic device (radius of 40 μm) is investigated and an increase in finesse and responsivity has been obtained. In our opinion, reducing the device dimensions, the imperfection and hence losses are reduced. Therefore, improved responsivity and finesse were expected. Of course, the low responsivity imposes photodetector to be connect to a suitable TIA whose gain can be chosen by taking into
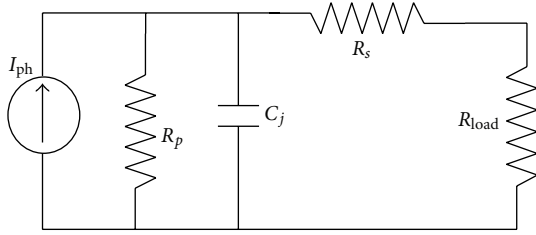
FIGURE 5: Equivalent circuit for small-signal analysis.

account the application field and the related performance requirements in terms of sensitivity and bandwidth.

3.4. Estimated Bandwidth. Figure 5 shows the equivalent circuit for small-signal analysis [25].

In the sketch, the photodetector schematized as a current generator (I_{ph}), the resistance (R_p) and capacitance (C_j) associated to the junction, the series resistance (R_s), and the load resistance (R_L) are reported. R_p (evaluated from the inverse derivative of the current-voltage characteristic) results in being greater than 60 kΩ at any reverse bias and 0.2 MΩ at −100 mV. On the other hand, R_s = 6.9 kΩ, extracted by fitting the I-V characteristic with the canonical equation of the Schottky diodes, results in being both much greater than load resistance (typically 50 Ω) and much smaller than parallel resistance R_p.

Hence, the device 3 dB frequency becomes

$$f_{3\,dB} = \frac{1}{2\pi R_s C_j}. \tag{2}$$

Finally, in order to estimate the bandwidth, the device capacitance has been measured by an LCZ meter (Keithley-3322) which drives the device with a known AC voltage input signal deriving the capacitance by precisely measuring the resultant current. The measured capacitance is smaller than 10 pF at any reverse bias and about 5 pF at −100 mV.

Unfortunately, the series resistance R_s is rather large due to the nonrectifying contact realized without a heavily p-doped region under the contact. For this reason, the estimated device bandwidth is limited to megahertz range but could be easily improved toward GHz operation in an optimized device provided a good ohmic contact.

4. IPE-Based Integrated Device

4.1. Proposed Device. The sketch of the proposed integrated device is shown in Figure 6, it is a rib waveguide fabricated starting from an SOI (silicon-on-insulator) substrate. The Cu Schottky metal is placed on the output facet, thus transversally to the optical field confined into the waveguide, while the collection contacts are placed on the waveguide slabs.

It is noteworthy that the Cu film on the bottom of the trench is deposited on the silicon oxide thick layer, thus the semiconductor/metal contact is only confined on the vertical surface of the trench. This allows to achieve a very narrow active region. On the other hand, the Cu layer on the oxide
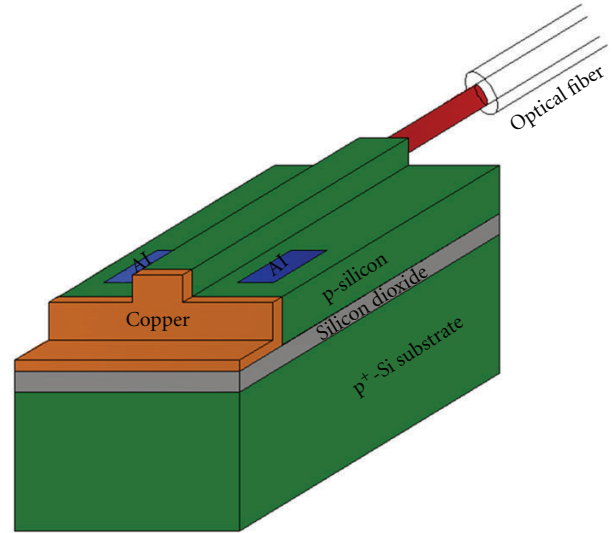

FIGURE 6: Schematic view of the proposed photodetector integrated with SOI waveguide.

layer provides a large region for the electrical pad contact without hampering the device capacitance.

4.2. Device Fabrication. In Figure 7, a top view of the proposed integrated photodetector is illustrated.

Rib waveguide was defined on a 1.5 μm thick lightly p-doped top layer of an SOI wafer with a 1.0 μm thick silicon oxide buried layer. The waveguide was formed by dry-etching the Si layer over a 100 nm depth, with a rib width of 2 μm. The rib height was chosen in order to assure a single mode propagation [29]. Alongside of the waveguides collecting ohmic contacts were placed; these contacts were realized by a thermally evaporated aluminium film, annealed at 475°C for 30 minutes. Waveguides were terminated on a deep trench that reaches down the buried oxide layer and formed by reactive ion etching (RIE). The thick photoresist, used as protection mask during trench etching, was not stripped after the RIE process, in this way a self-aligned lift-off process was performed to fabricate the Schottky contact by a 400 nm thick Cu layer, thermally evaporated on the vertical surface of the deep trench.

4.3. Responsivity Measurements. The photodetector responsivity has been measured by launching a light beam of a wavelength tunable laser source from a lensed optical fiber with a spot size of 3 μm into the SOI waveguide. The coupling and waveguide transmission loss have been evaluated by a numeric simulation [30], and a loss of about 6 dB has been estimated. A sourcemeter (Keithley-2410) was employed both to apply a bias voltage across the device and to measure the photogenerated current. Figure 8 illustrates the photogenerated current as function of the wavelength into a range from 1520 nm to 1620 nm at reverse bias of −1 V. At −1 V of the reverse bias applied, device dark current is about 0.01 μA.
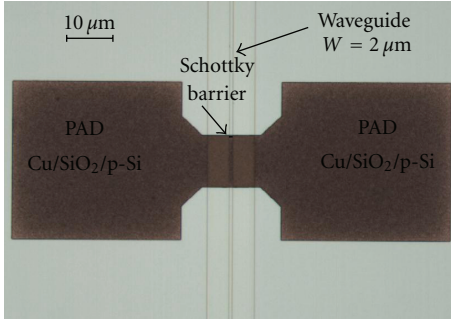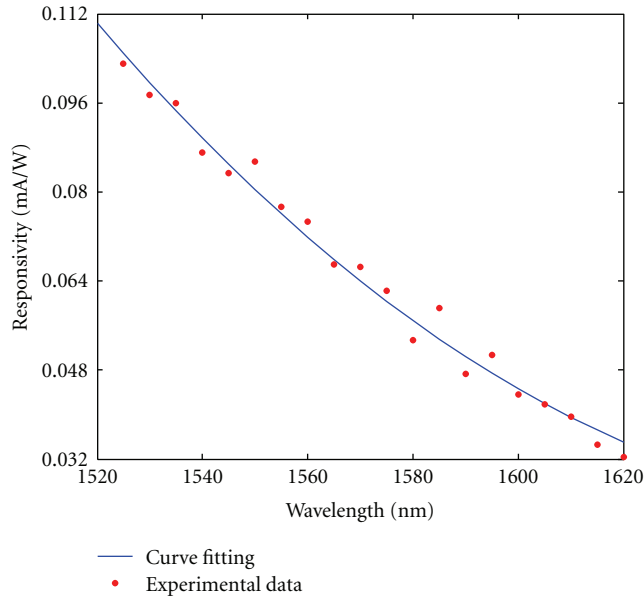
FIGURE 7: Top view of the proposed Si waveguide photodetector.

— Curve fitting
• Experimental data

FIGURE 8: Photogenerated current versus wavelength at -1 V of reverse bias applied.

The curve shows a downward trend with the optical wavelengths. This behaviour is typical for photocurrents generated by IPE and can be predicted by theoretical equation recalled in Section 2. Using it as curve fitting of the experimental data, the potential barrier has been extracted obtaining a value of $\Phi_B = 0.74 \pm 0.01$ eV. This confirms absorption due to the IPE and not to other mechanisms generating photocarrires as surface-state absorption or TPA whose behaviour, in terms of photogenerated current, grows by increasing the optical wavelengths [16].

4.4. Estimated Bandwidth. In order to estimate the bandwidth, the device capacitance has been measured by an LCZ meter (Keithley-3322) which drives the device with a known AC voltage input signal deriving the capacitance by precisely measuring the resultant current. The measured capacitance per unit area is about 4 fF/μm^2 at -1 V. Due to the large area of the Cu/p-Si interface of the characterized device (see Figure 7), its bandwidth is limited to megahertz range, in particular this area of 1.5 μm $\times$ 5 mm extends in much more

of the region around the waveguides, that is, of the active area useful for the photogeneration. However, in an optimized device the bandwidth could be easily improved by confining the Schottky interface strictly around the waveguide. If an active area for an optimized device of 1.5 μm (waveguide height) $\times$ 2 μm (waveguide width) is considered, a value of 12 fF for the capacitance can be estimated. It is noteworthy that when the detector area is made sufficiently small, the influence due to the capacitance is reduced and the effect of the transit time dominates [31]. The transit time limited bandwidth is given by

$$f_{tr} = \frac{0.44 v_{sat}}{W}, \tag{3}$$

where v_{sat} is the effective Si carrier saturation velocity (10^7 cm s^{-1}) and W is the depletion width. For a depletion width of 1.6 μm at reverse bias of -1 Volt [32], a bandwidth >170 GHz can be estimated.

5. Conclusions

In this paper the fabrication and characterization of all-silicon photodetectors based on IPE at 1550 μm have been reported. In particular, two types of structures, bulk and integrated devices, have been investigated.

Concerning the bulk photodetector, the preliminary device based on resonant structure exhibits a responsivity of about 8.2 μA/W around 1550 nm and the capacitance measurements (pF) encourage pursuing increased bandwidth toward GHz operation. Even if responsivity could be improved by optimizing a number of parameters, first of all the ohmic contact quality, its value could be still suitable for power monitoring applications. By comparing experimental results of this paper with the ones reported in our previous paper [28], we experimentally demonstrate that an improvement in responsivity can be obtained by increasing the cavity finesse. Hence, the proposed photodetector is thus very promising for integration in more complex microcavity having very high finesse (e.g., disk or ring resonator) which could allow the integration on silicon waveguide and a further enhancement in responsivity.
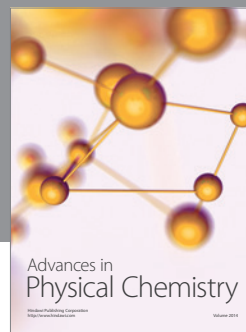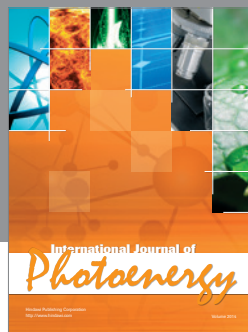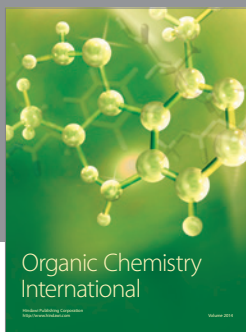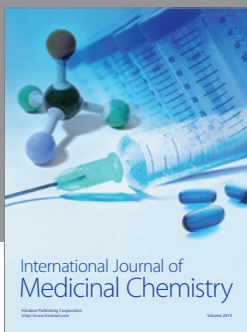
Concerning the integrated devices, the preliminary results exhibit a responsivity of 0.08 mA/W at 1550 nm and an efficient behaviour in both C and L bands.

In a next optimized device its responsivity could be enhanced by a resonant structure defined by etching deep trenches on the silicon rib waveguide. In addition, in order to obtain operation speed in the GHz range, the bandwidth could be improved by realizing a Schottky interface narrowly around the waveguide and by realizing a large pad for electrical contact and testing on the oxide.

References

[1] B. Jalali and S. Fathpour, "Silicon photonics," *Journal of Lightwave Technology*, vol. 24, no. 12, pp. 4600–4615, 2006.

[2] R. Soref, "The past, present, and future of silicon photonics," *IEEE Journal on Selected Topics in Quantum Electronics*, vol. 12, no. 6, pp. 1678–1687, 2006.

[3] L. Pavesi and D. Lockwood, *Silicon Photonics*, vol. 94 of *Topics in Applied Physics*, Springer, Berlin, Germany, 2004.

[4] L. C. Kimerling, L. dal Negro, S. Saini et al., "Monolithic silicon microphotonics," in *Silicon Photonics*, L. Pavesi and D. J. Lockwood, Eds., vol. 94 of *Topics in Applied Physics*, pp. 89–119, Springer, Berlin, Germany, 2004.

[5] L. K. Rowe, M. Elsey, N. G. Tarr, A. P. Knights, and E. Post, "CMOS-compatible optical rib waveguides defined by local oxidation of silicon," *Electronics Letters*, vol. 43, no. 7, pp. 392–393, 2007.

[6] L. Vivien, D. Pascal, S. Lardenois et al., "Light injection in SOI microwaveguides using high-efficiency grating couplers," *Journal of Lightwave Technology*, vol. 24, no. 10, pp. 3810–3815, 2006.

[7] Q. Xu, S. Manipatruni, B. Schmidt, J. Shakya, and M. Lipson, "12.5 Gbit/s carrier-injection-based silicon micro-ring silicon modulators," *Optics Express*, vol. 15, no. 2, pp. 430–436, 2007.

[8] C. P. Michael, M. Borselli, T. J. Johnson, C. Chrystal, and O. Painter, "An optical fiber-taper probe for wafer-scale microphotonic device characterization," *Optics Express*, vol. 15, no. 8, pp. 4745–4752, 2007.

[9] A. Liu, L. Liao, D. Rubin et al., "High-speed optical modulation based on carrier depletion in a silicon waveguide," *Optics Express*, vol. 15, no. 2, pp. 660–668, 2007.

[10] A. Liu, H. Rong, R. Jones, O. Cohen, D. Hak, and M. Paniccia, "Optical amplification and lasing by stimulated Raman scattering in silicon waveguides," *Journal of Lightwave Technology*, vol. 24, no. 3, pp. 1440–1455, 2006.

[11] G. Masini, L. Colace, and G. Assanto, "2.5 Gbit/s polycrystalline germanium-on-silicon photodetector operating from 1.3 to 1.55 μm," *Applied Physics Letters*, vol. 82, no. 15, pp. 2524–2526, 2003.

[12] L. Colace, P. Ferrara, G. Assanto, D. Fulgoni, and L. Nash, "Low dark-current germanium-on-silicon near-infrared detectors," *IEEE Photonics Technology Letters*, vol. 19, no. 22, pp. 1813–1815, 2007.

[13] M. Casalino, G. Coppola, M. Iodice, I. Rendina, and L. Sirleto, "Near-infrared sub-bandgap all-silicon photodetectors: state of the art and perspectives," *Sensors*, vol. 10, no. 12, pp. 10571–10600, 2010.

[14] T. K. Liang, H. K. Tsang, I. E. Day, J. Drake, A. P. Knights, and M. Asghari, "Silicon waveguide two-photon absorption detector at 1.5 μm wavelength for autocorrelation measurements," *Applied Physics Letters*, vol. 81, no. 7, pp. 1323–1325, 2002.

[15] J. D. B. Bradley, P. E. Jessop, and A. P. Knights, "Silicon waveguide-integrated optical power monitor with enhanced sensitivity at 1550 nm," *Applied Physics Letters*, vol. 86, no. 24, Article ID 241103, pp. 1–3, 2005.

[16] H. Chen, X. Luo, and A. W. Poon, "Cavity-enhanced photocurrent generation by 1.55 μm wavelengths linear absorption in a p-i-n diode embedded silicon microring resonator," *Applied Physics Letters*, vol. 81, Article ID 171111, 2009.

[17] S. Zhu, M. B. Yu, G. Q. Lo, and D. L. Kwong, "Near-infrared waveguide-based nickel silicide Schottky-barrier photodetector for optical communications," *Applied Physics Letters*, vol. 92, no. 8, Article ID 081103, 2008.

[18] A. Akbari and P. Berini, "Schottky contact surface-plasmon detector integrated with an asymmetric metal stripe waveguide," *Applied Physics Letters*, vol. 95, no. 2, Article ID 021104, 2009.

[19] Y. Wang, X. Su, Y. Zhu et al., "Photocurrent in Ag-Si photodiodes modulated by plasmonic nanopatterns," *Applied Physics Letters*, vol. 95, no. 24, Article ID 241106, 2009.

[20] R. H. Fowler, "The analysis of photoelectric sensitivity curves for clean metals at various temperatures," *Physical Review*, vol. 38, no. 1, pp. 45–56, 1931.

[21] V. E. Vickers, "Hydrostatic equilibrium and gravitational collapse of relativistic charged fluid balls," *Applied Optics*, vol. 10, pp. 2190–2192, 1971.

[22] E. Y. Chan and H. C. Card, "Near IR interband transitions and optical parameters of metal-germanium contacts," *Applied Optics*, vol. 19, no. 8, pp. 1309–1315, 1980.

[23] C. Scales and P. Berini, "Thin-film schottky barrier photodetector models," *IEEE Journal of Quantum Electronics*, vol. 46, no. 5, Article ID 5485040, pp. 633–643, 2010.

[24] H. C. Card, "Aluminum-silicon schottky barriers and ohmic contacts in integrated circuits," *IEEE Transactions on Electron Devices*, vol. ED-23, no. 6, pp. 538–544, 1976.

[25] S. Donati, *Photodetectors: Devices, Circuits, and Applications*, Prentice Hall PTR, Upper Saddle River, NJ, USA, 1999.

[26] M. S. Ünlü and S. Strite, "Resonant cavity enhanced photonic devices," *Journal of Applied Physics*, vol. 78, no. 2, pp. 607–639, 1995.

[27] E. D. Palik, *Handbook of Optical Constants of Solids*, Academic Press, San Diego, Calif, USA, 1985.

[28] M. Casalino, L. Sirleto, L. Moretti, M. Gioffré, G. Coppola, and I. Rendina, "Silicon resonant cavity enhanced photodetector based on the internal photoemission effect at 1.55 μm: fabrication and characterization," *Applied Physics Letters*, vol. 92, no. 25, Article ID 251104, 2008.

[29] S. P. Pogossian, L. Vescan, and A. Vonsovici, "The single-mode condition for semiconductor rib waveguides with large cross section," *Journal of Lightwave Technology*, vol. 16, no. 10, pp. 1851–1853, 1998.

[30] BeamPROP of RSoftDesignGroup, http://www.rsoftdesign.com/products.php?sub=Component+Design&itm=BeamPROP&det=Product+Overview.

[31] M. Casalino, L. Sirleto, L. Moretti, and I. Rendina, "A silicon compatible resonant cavity enhanced photodetector working at 1.55 νm," *Semiconductor Science and Technology*, vol. 23, no. 7, Article ID 075001, 2008.

[32] S. M. Sze, *Physics of Semiconductor Devices*, John Wiley & Sons, New York, NY, USA, 1981.